DOI:10.1021/jf1030967

JOURNAL OF AGRICULTURAL AND FOOD CHEMISTRY
ARTICLE

Thermodynamics of Grape and Wine Tannin Interaction with Polyproline: Implications for Red Wine Astringency

Jacqui M. McRae,[†] Robert J. Falconer,[‡] and James A. Kennedy*[,†,§]

[†]The Australian Wine Research Institute, PO Box 197, Glen Osmond SA 5064, Australia, and [‡]Australian Institute for Bioengineering and Nanotechnology, University of Queensland, St Lucia, QLD 4072, Australia. [§]Current address: California State University, Fresno, Department of Viticulture & Enology, 2360 E. Barstow Avenue MS VR89, Fresno, CA 93740-8003, USA

The astringency of red wine is largely due to the interaction between wine tannins and salivary proline-rich proteins and is known to change as wine ages. To further understand the mechanisms behind wine astringency change over time, thermodynamics of the interactions between poly(L-proline) (PLP) and grape seed and skin tannins (preveraison (PV) and commercially ripe) or Shiraz wine tannins (2 years old and 9−10 years old) was analyzed using isothermal titration calorimetry (ITC). The nature of these interactions varied with changes to the tannin structure that are associated with maturation. The change in enthalpy associated with hydrophobic interaction and hydrogen bonding decreased with tannin age and the stoichiometry of binding indicated that grape tannins associated with more proline residues than wine tannins, irrespective of molecular size. These results could provide an explanation for the observed change in wine astringency quality with age.

KEYWORDS: Astringency; ITC; proline; protein−tannin interactions; tannin; wine age

INTRODUCTION

Astringency is an important feature of red wine and has a significant role in its overall quality (*1*). With age, red wines often transform from a harsh, puckering astringency to that which is considered softer (*2*). The explanation for this change remains unknown. Possible explanations for this phenomenon have included a decrease in the concentration of tannins in solution via polymerization and subsequent precipitation, tannin removal through fining with residual proteins in the wine matrix or tannin degradation through cleavage reactions (*3*−*6*). The tannin concentrations of aged wines have been observed to be similar to those of young wines, suggesting that tannin structural changes play a role (*7*). Tannins are extracted from grape skins and seeds during wine making (*8*), and these condensed tannins are generally composed of catechin (**1**), epicatechin (**2**), epicatechin 3-*O*-gallate (**3**) and epigallocatechin (**4**) subunits (**Figure 1**) linked with C4−C8 or C4−C6 interflavan bonds (*9*−*11*). Skin tannins contain epigallocatechin subunits and generally have a low proportion of epicatechin 3-*O*-gallate while seed tannins lack epigallocatechin and contain a comparatively high proportion of epicatechin 3-*O*-gallate (*10*). During fermentation, maceration, and subsequent wine aging, modification of tannin structures occurs, and a major focus of wine chemistry is to elucidate the reactions that lead to structure modifications (*9*, *12*). For example, direct condensation reactions produce tannin−anthocyanin (T−A) and A−T adducts, resulting in pigmented polymers (*13*), while indirect condensation reactions involve the mediation of condensed tannin polymerization by oxidation products in the wine matrix, such as acetaldehyde, resulting in tannins with modified interflavan bonds. Some resulting compounds, such as ethyl-linked polymers, are unstable and undergo further reaction (*5*, *9*). Stable pigments, such as pyranoanthocyanins, also form from anthocyanins, including malvidin 3-glucoside (**5**), and can be incorporated into the tannin structure (*14*, *15*). In addition, continued gradual oxidation over time is thought to alter the structure of tannins (*15*, *16*). Previous reports have indicated that pigmented polymer formation reduces the perception of astringency (*1*), hence changes to the structure of tannins are likely to influence their sensory properties.

The sensation of astringency is produced largely from the loss of lubrication in the oral cavity as a result of interaction and subsequent precipitation between wine tannins and salivary proteins, particularly proline-rich proteins (PRPs) (*17*). This interaction occurs over different stages and involves a combination of hydrophobic interactions and hydrogen bonding (**Figure 2**). In the initial interaction, hydrophobic ($\pi-\pi$) associations occur between the planar surfaces of the tannin aromatic rings and the heterocyclic proline ring of PRPs, and hydrogen bonding occurs between the acidic protons of the tannin and the polar amino acid residues of proline residues. The relative contribution of each may vary due to the structure of the condensed tannin. The interaction between procyanidin B2 (epicatechin-(4α-8)-epicatechin) and 19-residue poly(L-proline) (PLP) was found to be initiated by hydrophobic interactions (*18*); however, investigations of procyanidin B3 with a human salivary protein fragment (*19*) indicated that initial interactions through hydrogen bonds are important. These differences in mechanism of interaction may be due to variations in tannin conformation, favoring either the compact or extended forms, which impacts upon the

*Corresponding author. Tel: +1 559 278 2089. Fax: +1 559 278 4795. E-mail: jakennedy@csufresno.edu.

 Published on Web 11/11/2010

type of available binding sites on the tannin (*20*). In secondary interactions, protein−tannin complexes self-associate via further hydrogen bonding to produce larger protein−tannin complexes, which then aggregate and subsequently precipitate from solution (*21*).

Differences in binding between PLP and catechin derivatives have been successfully demonstrated using isothermal titration calorimetry (ITC) (*22*), and this technique has also been used to measure differences in polymer interactions with membranes (*23*). In this study, PLP−tannin interactions were assessed for tannins isolated from aged wine, young wine and grapes, in order to better understand how tannin interaction with proteins varies with wine age.

MATERIALS AND METHODS

Wine and Grape Samples. Six Australian Shiraz samples were sourced from a wine cellar (Edinburgh Cellars, Adelaide, South Australia). The wines were from different wineries and different grape growing regions within South Australia, and included three 2007 vintage wines (2007A, 2007B, and 2007C), two 2000 vintage wines (2000A and 2000B), and one 1999 vintage wine (1999). Preveraison (PV) *Vitis vinifera* L. cv. Tannat grapes and commercially ripe (CR) cv. Shiraz were collected from a separate vineyard from the wine samples. The seeds and skins were separated prior to extraction.

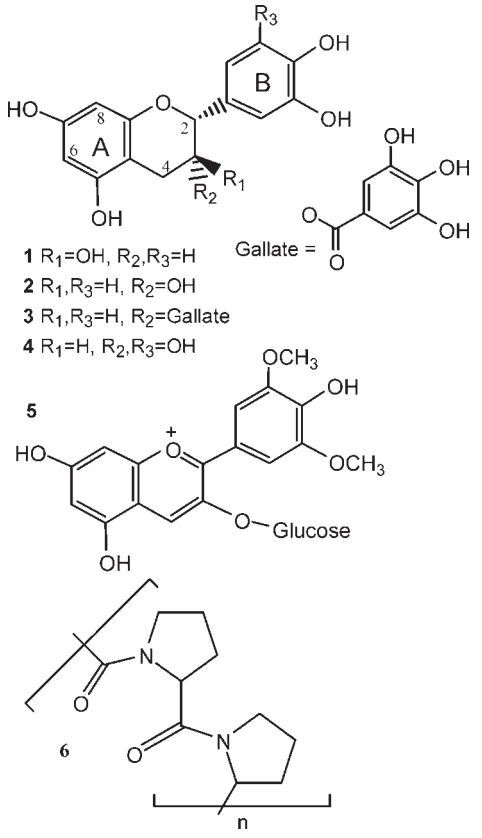

Figure 1. Structures of tannin subunits (**1**−**4**), malvidin-3-glucoside (**5**) and poly(L-proline) (**6**).

Wine Characterization. The basic wine chemistry for each sample was determined using a *FOSS* WineScan (FT-120) rapid-scanning infrared Fourier-transform spectrometer with *FOSS* WineScan software Version 2.2.1 (P/N 1010968), analyzing for alcohol concentration, pH, specific gravity, titratable acidity at pH 8.2 and 7.0, glucose and fructose concentration and volatile acidity as acetic acid.

Tannin Isolation. Tannin was isolated from wine as reported by Kennedy and Jones (*24*). Briefly, a glass column packed with 500 mL of Toyopearl HW-40C (Sigma, Castle Hill, NSW, Australia) was equilibrated with H_2O/0.01% v/v TFA prior to loading 400 mL of wine. The column was washed with H_2O/0.01% v/v TFA (2 L), followed by 1:1 MeOH:H_2O containing 0.01% v/v TFA (8 L) at 18 mL/min. Tannin was eluted using 2:1 acetone:H_2O containing 0.01% v/v TFA (2 L). The acetone was removed under vacuum using a rotary evaporator at 30 °C, and the aqueous residue was removed by freeze-drying. The tannin samples were then stored at −80 °C. The gravimetric recovery of wine tannin was recorded: 2007A, 1553.9 mg/L; 2007B, 1676.1 mg/L; 2007C, 1640.3 mg/L; 2000A, 1253.3 mg/L; 2000B, 1314.5 mg/L; 1999, 1735.2 mg/L. Tannin was also extracted from preveraison and commercially ripe grape seed and skins using 2:1 acetone:H_2O containing 0.01% v/v TFA and was purified using Toyopearl chromatography media as per Bindon et al. (*25*).

Tannin Characterization. The composition of the isolated tannins was characterized using acid catalysis in the presence of excess phloroglucinol (phloroglucinolysis) as per Kennedy and Jones (*24*) with slight modifications, and the molecular size of each sample was estimated using gel permeation chromatography (GPC) (*26*). For phloroglucinolysis, tannins were dissolved in MeOH to 10 g/L and 25 μL was reacted with 25 μL of phloroglucinol solution (phloroglucinol (100 g/L) in MeOH with 20 g/L ascorbic acid and 0.2 N HCl) at 50 °C for 25 min. Sodium acetate solution (70 mM, 150 μL) was added, and the reaction products were analyzed using HPLC with a Wakosil RPC18 column (200 × 2 mm) at 25 °C and a mobile phase of 95:5 1% v/v acetic acid/MeOH with a gradient to 100% MeOH over 80 min at 1 mL/min and monitoring at 280 nm. The chromatogram peaks were integrated and the proportions of flavan-3-ol monomers were calculated as per Kennedy and Jones (*24*).

This procedure enabled the identification of flavan-3-ol subunits within the tannin that were linked via acid-labile interflavan bonds. The calculated mass of these subunits was then compared to the original tannin mass (determined gravimetrically), and the difference between the mass of tannin in the sample and the calculated mass of the comprising subunits gave the percent mass conversion. The presence of subunits other than catechin derivatives, including anthocyanins and their derivatives, and the presence of non-acid-labile interflavan bonds were not identified using this method. Thus tannins with greater proportions of these structural characteristics demonstrated lower mass conversions.

For GPC, 80 μL of *N*,*N*-dimethylformamide (DMF) was added to 20 μL of tannin in MeOH to a final tannin concentration of 2 g/L. Samples were analyzed using two PLgel columns (300 × 7.5 mm, 5 μm, 100 Å followed

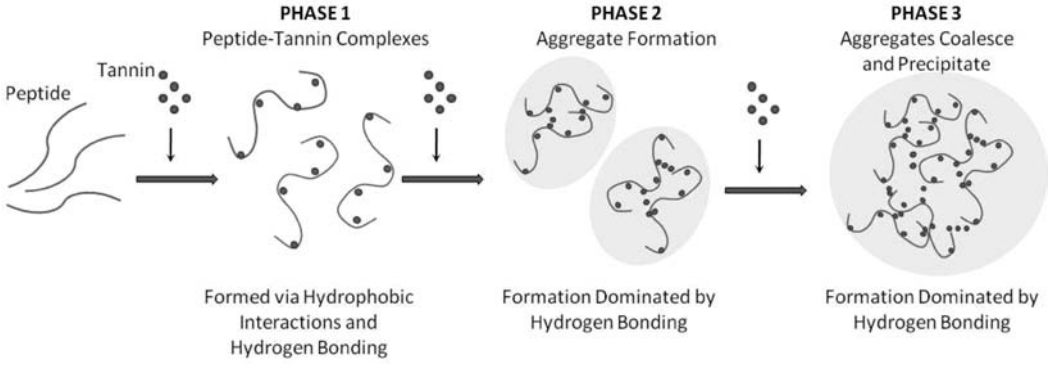

Figure 2. Summary of the main phases of peptide−tannin interactions and the major mechanisms of interaction (*17*).

by 500 Å) connected in series and protected by a guard column containing the same material (50 × 7.5 mm, 5 μm), all purchased from Polymer Laboratories (Amherst, MA, USA), and a mobile phase of DMF with 0.15M LiCl, 5% v/v water, and 1% v/v acetic acid. Chromatograms were analyzed using Agilent ChemStation software against a standard curve of fractionated preveraison (PV) grape proanthocyanidins with their molecular mass determined by phloroglucinolysis as per Kennedy and Taylor (*26*). This method estimated the molecular mass distribution of the tannin by comparing the GPC elution profile to that of tannin with a known average molecular mass (PV seed tannin or PV skin tannin for all skin and wine tannins). The extent of coloration for each tannin sample was determined by comparing the peak area at 520 nm to that at 280 nm.

Peptide−Tannin Affinity Assays. Peptide affinity assays were performed using a modification of the MCP assay (*7*). Tannin solutions (4 g/L in 1:9 EtOH/10 mM ammonium formate buffer, pH 3.5, 25 μL) were reacted with 300 μL of poly(L-proline) solution (PLP, molecular mass 5600 Da; DPn 58, Sigma-Aldrich, 40 μM in ammonium formate buffer) in a 96 well plate for 3 min. Saturated ammonium sulfate solution (200 μL, Sigma-Aldrich) was added to each reaction, and the plate was shaken for 1 min and allowed to sit for 10 min. The plate was then centrifuged, the supernatant transferred to a UV plate and the absorbance measured at 280 and 520 nm using a Molecular Devices SpectraMax M2 microplate reader.

Isothermal Titration Calorimetry (ITC). ITC was undertaken with an ITC200 (MicroCal, Northampton, MA, USA). The titrant was 2 mM of isolated tannin from either grapes or wine, calculated using the determined extinction coefficients (**Table 2**), dissolved in EtOH and then diluted 1:9 with 11 mM ammonium acetate, pH 4.0. To calculate the extinction coefficients, a solution containing a known gravimetric concentration of each tannin sample was serially diluted using ammonium acetate buffer, and the absorbance of the resulting solutions was determined using a microplate reader at 280 nm (Molecular Devices SpectraMax M2). The molar concentrations of the tannin solutions were then calculated based on the average molecular weight of each isolated tannin as determined by GPC and plotted against absorbance to give the extinction coefficient of each tannin. The sample cell contained 100 μM PLP dissolved in 10 mM ammonium acetate, 10% (v/v) EtOH at pH 4.0. The titration comprised 17 × 2 μL injections at 25 °C unless otherwise stated. To differentiate between hydrophobic interaction and hydrogen-bonding driven binding, the temperature of the reaction was operated at 10, 20, 25, 35, 45, and 55 °C. The ΔH of binding is temperature dependent for hydrophobic interaction-driven binding (*27*).

Data analysis used the Origin 5.0 software package (ITC Data Analysis in Origin, MAU130010 REV F-4, Microcal, Northampton, MA, USA). The binding constant, K, and change in Gibbs free energy were calculated as previously reported (*27*, *28*). The model that was used calculate the stoichiometry, association constant, ΔH, $T\Delta S$ and ΔG was based on a "single set of identical sites" provided by the Origin 5.0 software package (*28*). Control injection of tannins into 10 mM ammonium acetate, 10% (v/v) EtOH at pH 4.0 solution (without PLP) showed negligible ΔH. For the titration at different temperatures the baseline had to be adjusted to take into account the temperature difference of the titrant to the sample. Nonlinear least-squares curve fitting was used (ITC Data Analysis in Origin). All errors shown in the paper are based on the accuracy of the curve fit to the data.

Statistical Analysis. All significance tests (ANOVA and Student's t tests) were conducted using the JMP 5.0.1 statistics software. Results have been incorporated into the tables.

RESULTS AND DISCUSSION

Wine Characterization. The selected Australian wine samples covered vintages from 2007, 2000, and 1999. Analysis using *FOSS* WineScan analysis (**Table 1**) provided basic chemical information, including pH, ethanol concentration, specific gravity, glucose/fructose concentrations and the titratable and volatile acidity. The overall results for each wine were similar, with a pH range from 3.40 to 3.64 and an average EtOH concentration of 14.3 ± 0.47% (one standard deviation). There were no distinctive trends for the titratable acidity or sugar concentrations, although a slight trend was observed for volatile acidity with the average young wine concentration of 0.63 ± 0.03 g/L being slightly higher than the 0.55 ± 0.02 g/L observed for aged wine. Tannin concentration in the wine was varied across all samples, indicating that the softening of wine astringency over time is unlikely to be due solely to a decrease in tannin concentration.

Table 1. Properties of the Selected Shiraz Wine Samples

wine param tested	2007A	2007B	2007C	1999	2000A	2000B
ethanol (% v/v)	14.1	14.7	14.5	13.6	14.2	14.9
sp gravity	0.9938	0.9947	0.9943	0.9937	0.9939	0.9930
pH	3.50	3.43	3.64	3.50	3.51	3.40
titratable acid (g/L)						
pH 8.2	6.2	6.2	6.3	6.3	6.5	5.9
pH 7.0	5.5	6.9	5.7	5.7	5.9	5.4
glucose + fructose (g/L)	1.1	0.6	0.4	0.2	<0.27	0.7
volatile acidity (g/L)[a]	0.66	0.63	0.61	0.56	0.56	0.53
tannin concn (mg/L)	1553.9	1676.1	1640.3	1735.2	1253.3	1314.5

[a] Measured as acetic acid.

Table 2. Phloroglucinol and GPC Analysis Results for Isolated Grape and Wine Tannins

	% MC[a]	mDP[b]	% tri-OH[c]	% gallate[d]	MW[e]	% $A_{520/280}$[f]	ε ($\times 10^3$)[g]
PV seed	71.6	6.8	0	19.5	2721	na[h]	43.0
PV skin	78.3	15.7	24.7	2.4	5271	na	75.5
CR seed	78.3	4.85	0	23.7	2902	na	48.3
CR skin	49.9	31.9	47.3	5.3	6491	3.8	122.7
2007A	28.8	8.45	16.8	5.3	2726	14.6	33.8
2007B	29.1	10.73	29.9	3.8	3549	15.9	38.8
2007C	18.7	11	29.3	3.2	3399	15.1	33.6
av	25.5 a	10.1 a	25.3 a	4.1 a	3225 a	15.2 a	35.4 a
young wine[i]	±5.9	±1.4	±7.4	±1.1	±438	±0.7	±2.9
1999	6.6	6.28	23.4	5.3	4190	18.6	55.2
2000 A	9.1	7.49	25	2.7	3504	17.8	48.6
2000 B	5.2	7.07	24.5	3.5	5218	17.1	73.0
av	7.0 b	6.9 b	24.3 a	3.8 a	4304 a	17.8 b	58.9 b
aged wine[i]	±2.0	±0.6	±0.8	±1.3	±863	±0.8	±12.6

[a] MC, mass conversion. [b] mDP, mean degree of polymerization. [c] % tri-OH, percent epigallocatechin. [d] % gallate, percent epicatechin gallate. [e] MW, average molecular weight obtained from the 50% GPC elution. [f] % $A_{520/280}$, percent of absorbance at 520 nm compared with 280 nm. [g] ε, extinction coefficients (M^{-1} cm^{-1}). [h] na, not applicable for these samples as colored anthocyanins were not present in the tannin. [i] Averaged results are shown ± one standard deviation of the mean, and results in the same column with different letters (a, b) are significantly different ($p < 0.05$).

Tannin Characterization. Acid-catalyzed cleavage of the isolated tannins in the presence of phloroglucinol and subsequent HPLC analysis demonstrated structural differences between young and aged wine tannins as well as between grape skin and seed tannins (**Table 2**). The variation between the skin and seed tannin composition demonstrated the expected characteristics with regard to epigallocatechin and epicatechin-3-*O*-gallate proportions as previously noted (*10*, *11*). For the wine tannin samples, no trend was observed in the proportion of epigallocatechin subunits (% tri-OH) and galloylated subunits (% gallate) with averages of 24.8 ± 4.7% and 4.0 ± 1.1%, respectively. The extent of pigmentation in the tannins was estimated by measuring the total peak area for each tannin sample in the GPC chromatograms at 520 nm relative to 280 nm. The retention time of the colored tannin was measured relative to a malvidin-3-glucoside standard to ensure the 520 nm absorbance was not due to the presence of free anthocyanins. The aged tannins exhibited a slightly greater proportion of red coloring than the young wine tannin ($A_{520/280}$ 17.8 ± 0.8% and 15.2 ± 0.7%, respectively), suggesting that these samples contained a higher proportion of the flavylium form of anthocyanin. This is consistent with the

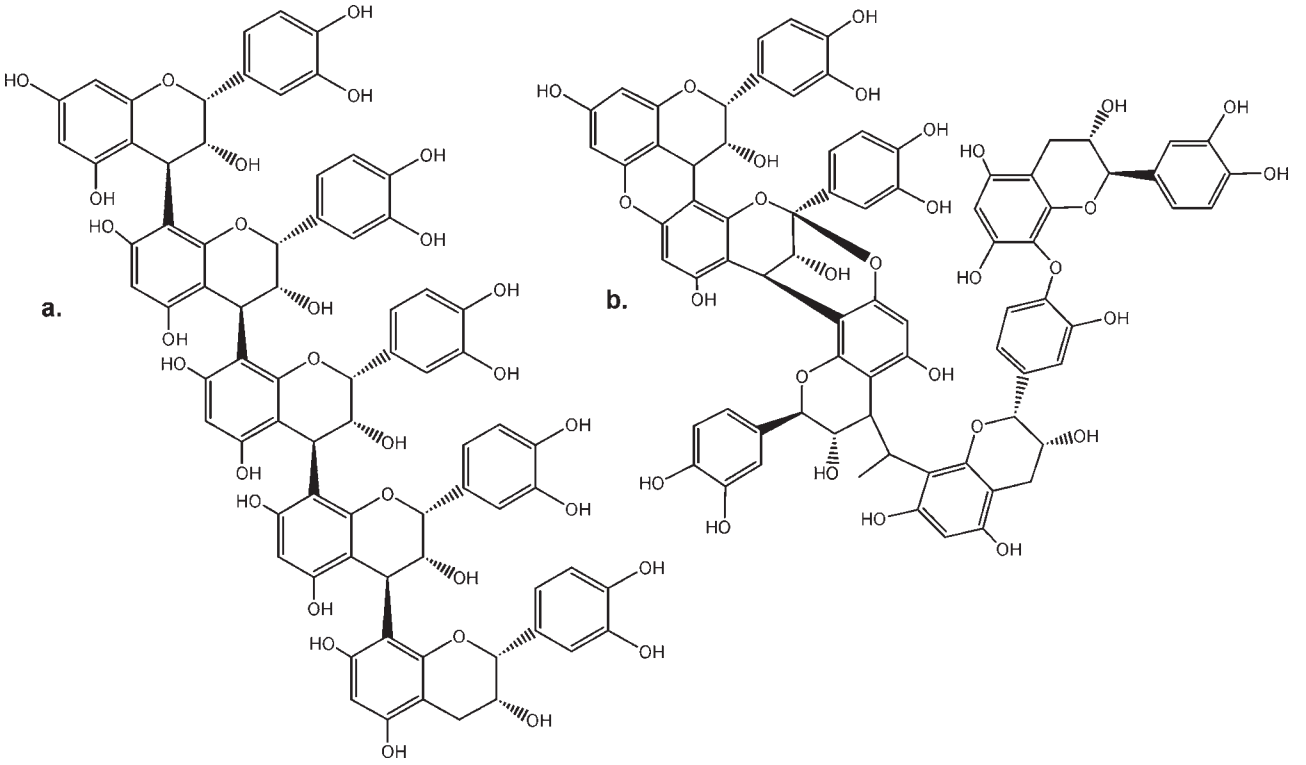

Figure 3. Hypothetical representations of PV grape tannins (**a**) and aged wine tannins (**b**), demonstrating the impact of interflavan bond modifications on the resulting tannin structure (*15*, *16*).

observed reduction in free anthocyanin concentrations in the aged wine samples compared with the young wine samples as mentioned above, as well as suggestions that the concentration of free anthocyanins in wine is reduced as anthocyanin−tannin adducts form (*15*).

The low mass conversion of the wine tannins as determined by phloroglucinolysis indicated that only a small proportion of the tannin could be characterized using this method. As such, the determined mean degree of polymerization (mDP) for each tannin sample and thus the molecular mass calculated by phloroglucinolysis is unlikely to be reliable for these samples. Thus the average molecular mass of each sample was determined by comparing the GPC elution time of the sample tannin at 50% to that of PV grape tannins of known molecular mass and higher mass conversion value. It was considered that this approach would provide a more accurate determination of the molecular mass of each sample. These results indicated that the molecular mass of aged wine tannin was generally, but not significantly, higher than that of young wine tannin (4304 ± 862 compared with 3225 ± 438) (**Table 2**).

Effect of Age on Wine and Grape Tannin Structure. The structures of grape and wine tannins become increasingly modified with age. Preveraison (PV) grape tannins are composed largely of flavan-3-ol subunits with 4-8 or 4-6 (B-type) interflavan bonds, as demonstrated by the high mass conversion and subunit composition determined with phloroglucinolysis (**Table 2**). As the grapes ripen, there is an apparent oxidation of seed tannins, and some anthocyanins may be incorporated into skin tannins (*10*). Crushing and fermentation of grapes and subsequent aging of wine expose the extracted grape tannins to oxidative conditions (*3*), which can convert polyphenols into highly reactive quinones (*9*). This results in the polymerization of tannins via the addition of subunits, and the formation of modified interflavan bonds including 4-6,2-*O*-7 interflavan bonds (A-type linkages) and ether linkages formed from the B-ring hydroxyl groups (*29*, *30*). The greater polymerization and alteration of interflavan bonds produces an increase in tannin hydrophobicity over time (*31*). Tannins in aqueous solution form a mixture of extended and compact configurations where the latter is the dominant form for most dimers and trimers, and therefore the greater polymerization is likely to lead to a folding of tannin subunits resulting in increased intramolecular associations (*32*). The changes in tannin structure that occur as a result of oxidation are observed as a decrease in mass conversion due to the formation of interflavan bonds that are not susceptible to acid-catalyzed cleavage (7.0 ± 2.0% for aged wine tannins compared with (25.5 ± 5.9% for young wine tannins). This increases the deviation between the apparent molecular mass as determined by phloroglucinolysis and that determined by GPC as the wine ages. Increased anthocyanin content of the tannin would account for some of the reduction in mass conversion; however, it is likely that the changes in wine tannin structure are mostly due to oxidation. Hence as wine tannins age, the chemical changes described above are likely to result in a larger and more folded structure compared to PV grape tannin (**Figure 3**).

Peptide−Tannin Affinity Assays. As tannins age, tannin size and hydrophobicity are thought to increase as a result of tannin oxidation, and theoretically this would increase protein affinity (*31*). However, this is contrary to the reported reduction in astringency of red wine as it ages. Initial peptide−tannin affinity assays were conducted to determine any differences in observed PLP interactions between aged and young wine tannins as well as PV and commercially ripe (CR) grape tannins. Tannin-containing model wines were prepared at the same gravimetric concentration and then reacted with 40 μM PLP to precipitate all of the tannins from solution. The amount of tannin precipitated as measured by the change in absorbance at 280 nm was similar for all tannin samples, indicating no difference in PLP interaction (data not shown). Structural differences in flavan-3-ol monomers have previously been shown to result in changes in protein

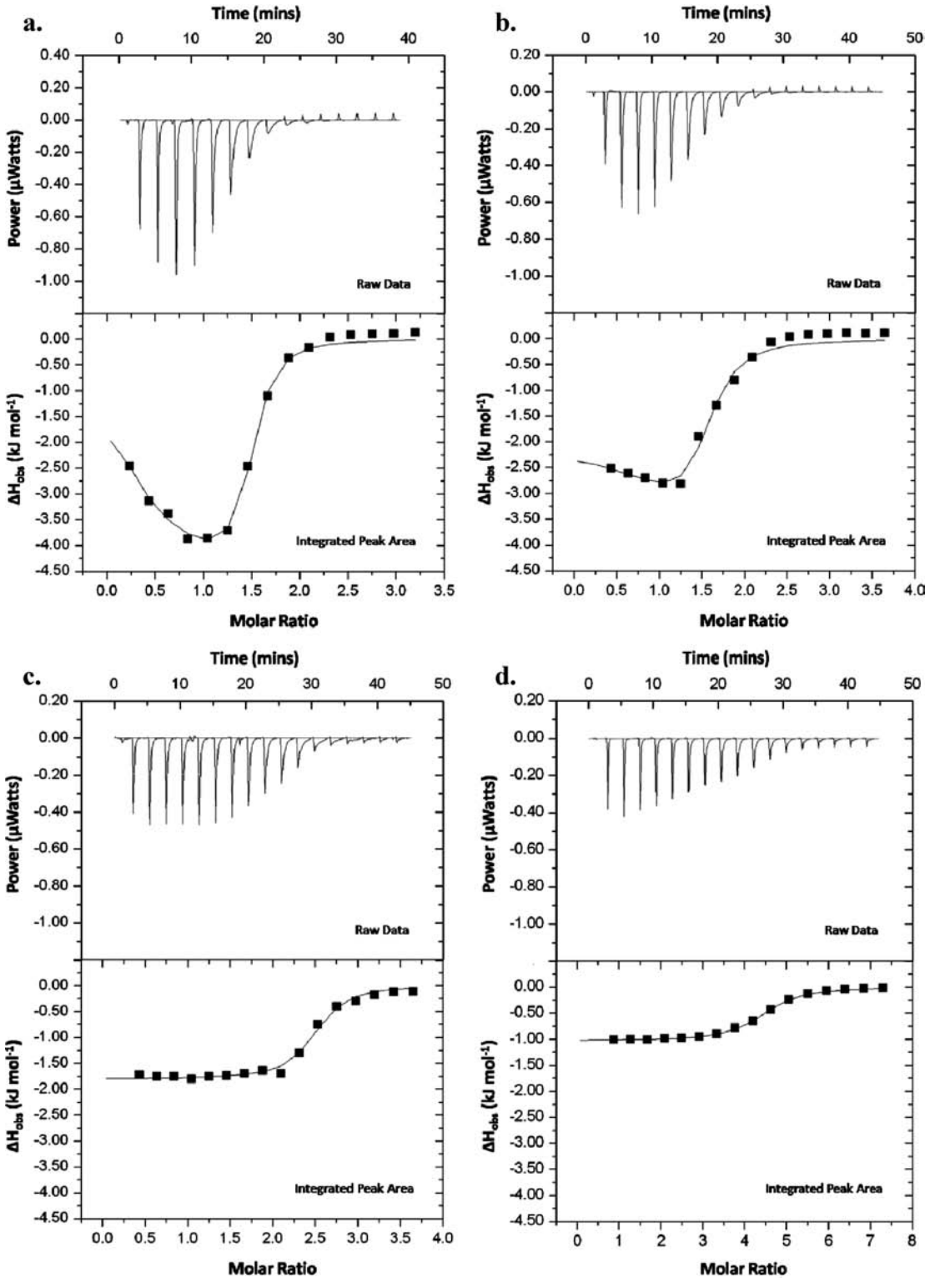

Figure 4. Interaction of (**a**) preveraison skin tannin, (**b**) commercially ripe skin tannin, (**c**) young wine tannin (2007A), and (**d**) aged wine tannin (2000A) with polyproline studied by ITC at 25 °C showing the thermogram and binding isotherm.

interactions when measured by isothermal titration calorimetry (ITC) (*33*), and therefore ITC was used to measure changes in the interaction between different tannin samples and PLP.

Isothermal Titration Calorimetry. The ITC curves of tannin extracts titrated into PLP solutions are shown in **Figure 4**. From the titration curves the change in enthalpy (ΔH) was calculated from the area under each curve, the stoichiometry and the binding association constants (K) were determined from the shape of the curve, and from this the change in Gibbs free energy (ΔG) and change in entropy (ΔS) were calculated (*34*) and are shown in **Table 3**. The interaction between macromolecules is highly complex, and the interpretation of thermodynamic changes is therefore necessarily generalized (*35*). The measured negative ΔH for the titration of a tannin solution into a PLP solution is often associated with exothermic hydrogen bonding, which may occur between tannins and PLP to form complexes in the first phase of

Table 3. Thermodynamic Parameters for Interaction of Grape and Wine Tannins with PLP Including the Stoichiometry (n), Association Constant (K), Change in Enthalpy (ΔH) and Change in Entropy (ΔS)[a]

	n	K ($\times 10^6$)	ΔH (kJ/mol)	$T\Delta S$ (kJ/mol)	MW
PV seed	2.13 ± 0.02	0.25 ± 0.03	−63.8 ± 1.3	−32.2	2721
PV skin	1.44 ± 0.02	1.22 ± 0.33	−71.0 ± 1.8	−36.1	5271
CR seed	1.83 ± 0.03	0.70 ± 0.25	−51.3 ± 1.3	−17.6	2902
CR skin	1.52 ± 0.04	0.47 ± 0.20	−54.8 ± 4.0	−22.4	6491
2007A	2.41 ± 0.02	0.76 ± 0.18	−31.5 ± 0.5	2.1	2726
2007B	2.45 ± 0.02	1.10 ± 0.23	−30.2 ± 0.4	4.4	3549
2007C	2.46 ± 0.01	0.53 ± 0.05	−28.8 ± 0.3	3.9	3399
1999	2.62 ± 0.03	0.59 ± 0.17	−19.8 ± 0.5	12.5	4190
2000A	4.3 ± 0.02	0.42 ± 0.03	−18.0 ± 1.1	13.7	3504
2000B	1.98 ± 0.02	0.35 ± 0.04	−30.3 ± 0.5	1.3	5218

[a] Derived by fitting a single binding site model. The average molecular weights (MW) as determined by GPC are included for comparison.

association or between complexes to form aggregates as in the second phase of association (**Figure 2**) (*33*). The ΔS has been attributed to conformational changes in PLP and tannins (though both of these molecules are reasonably rigid) and the displacement of water molecules as a result of hydrophobic interactions (*33*, *34*).

Hydrophobic Interactions and Hydrogen Bonding. The influence of hydrogen bond formation or hydrophobic interactions on the ITC titration curve was studied by repeating the PLP−PV seed tannin experiment at 10, 20, 25, 35, 45, and 55 °C (**Figure 5**). The initial binding reaction that occurred between 0 and 1.0 molar ratio was substantially altered by the change in temperature; however, there was no change in the subsequent binding reaction that took place at molar ratios greater than 1.0. The shape of the initial part of the titration curve suggests that there are competing exothermic and endothermic binding interactions taking place. The strength of the endothermic component (positive ΔH) of this binding reaction increased with rising temperature. This is consistent with hydrophobic interaction. This is due to the structured water around apolar residues having a higher heat capacity than the bulk water. As hydrophobic interaction takes place, structured water is displaced, changing the heat capacity (ΔC_p). As $\Delta C_p = \delta\Delta H/\delta T$ (*34*), the change in heat capacity is observed as a change in enthalpy with change in temperature, as observed in this experiment. The differences in the titration curves as well as the calculated changes in enthalpy for each tannin sample demonstrated the impact of structural differences to the tannin on PLP interaction. Initial hydrophobic interactions were most pronounced for the PV grape tannins with comparatively large negative enthalpy change observed at molar ratios of less than 1.0. These interactions were less pronounced for the other tannin samples.

The second part of the titration curve that is evident at molar ratios greater than 1.0 was resistant to changes in temperature, and analysis of this section of the curve demonstrated consistent n, K, ΔH and ΔS values over this temperature range. This was consistent with interactions that are predominantly facilitated by bonding other than hydrophobic interactions and therefore can be assumed to be hydrogen bonding, possibly supplemented with van der Waals forces. The hydrophobic interaction sites on the PLP in the sample cell became saturated with tannin at concentrations greater than approximately 1.0 molar ratio, forming metastable aggregates of tannin−PLP complexes via hydrogen bonds.

The interaction of PLP with tannins was shown to be due to both hydrophobic interactions and hydrogen bonding, and the relative contribution of each type of association was dependent on tannin structure. The relationships between the relative molecular sizes of the tannins (calculated as a molecular weight from the GPC 50% elution time) and the ΔH and $T\Delta S$ are shown in **Figure 6**. PV grape tannins exhibited a greater interaction with PLP, demonstrated by the initial increase in exothermic reactions (negative ΔH) in the titration curves, by the large negative ΔH associated with greater energy release, and by the large and negative ΔS (**Table 3**), which suggested that both hydrophobic interactions and hydrogen bonding were essential for the formation of PLP−PV grape tannin complexes (*34*). This trend seemed independent of the relative molecular sizes of the seed and skin tannins. The initial negative trend in ΔH in the titration curves of the CR grape tannins was less pronounced than for the PV grape tannins, and the overall ΔH and ΔS decreased, suggesting that the hydrophobic interaction was less extensive than with the PV grape tannin interactions. The molecular weight of the CR skin tannin was substantially larger than that of the CR seed tannin (6491 and 2902, respectively) and yet the ΔH was similar, demonstrating that structural modifications of the ripe skin tannin, such as the incorporation of anthocyanins (*10*), reduced the PLP interactions.

The negative ΔH decreased further in young wine tannins compared to tannins extracted from grape presumably as a result of structure modification of extracted grape tannins. Aged wine tannins demonstrated the smallest negative ΔH, despite an increase in molecular size. The weak positive entropy change demonstrated by the wine tannins was possibly associated with expulsion of some water from the surface during PLP−tannin complex formation.

The impact of hydrophobic interactions was least pronounced in the aged wine tannins, where there was little evidence of endothermic contribution to the titration curve. The relatively weakly negative change in enthalpy is probably due to binding events with fewer hydrogen bonds in the complex aged wine tannins. The change in entropy of the largest aged wine tannin, 2000B, was similar to that of the young wine tannins. This sample had the largest average molecular size of the wine tannins; however the ΔH was similar to that of the much smaller younger wine tannins (**Figure 6**). This suggests that the greater interaction that should have been exhibited by the larger tannin has been counteracted by the presumed tannin modification with age (*15*, *16*).

Stoichiometry and Binding Constants. The thermodynamic parameters were calculated for each tannin sample based upon the ITC titration curves using the single set of identical sites model (**Table 3**). The binding association constants were similar for all samples irrespective of different molecular sizes of the compounds; however, the stoichiometry (n) demonstrated differences in how the tannins bound to PLP. The n value was generally inversely proportional to the molecular mass as expected, yet PV skin tannin bound to only 1.5 times the number of proline units (assuming an average DP for PLP of 58) as PV seed tannin despite being 1.9 times the GPC-determined molecular mass. This may be due to size−molecular mass relationships between skin and seed tannin as noted previously (*18*, *25*, *32*), although steric hindrance may also limit the binding ability of the larger tannin. CR skin tannin contained a higher proportion of anthocyanins than CR seed tannin (*10*), which has previously been shown to have little or no contribution to the astringency of model wine (*1*). In this experiment, CR skin tannin was 2.2 times the size of CR seed tannin, and yet it bound to only 1.2 times as many proline units, suggesting that the incorporation of anthocyanins into the tannin structure may decrease the association of the tannin with PLP. The aged wine tannin bound to fewer proline units than the young wine tannin at a similar molecular mass, and likewise, young wine tannin associated with fewer proline residues than the CR grape tannin. This gives further indication that intramolecular associations produced by the larger and more oxidized tannins hinder the number of binding sites available for PLP association.

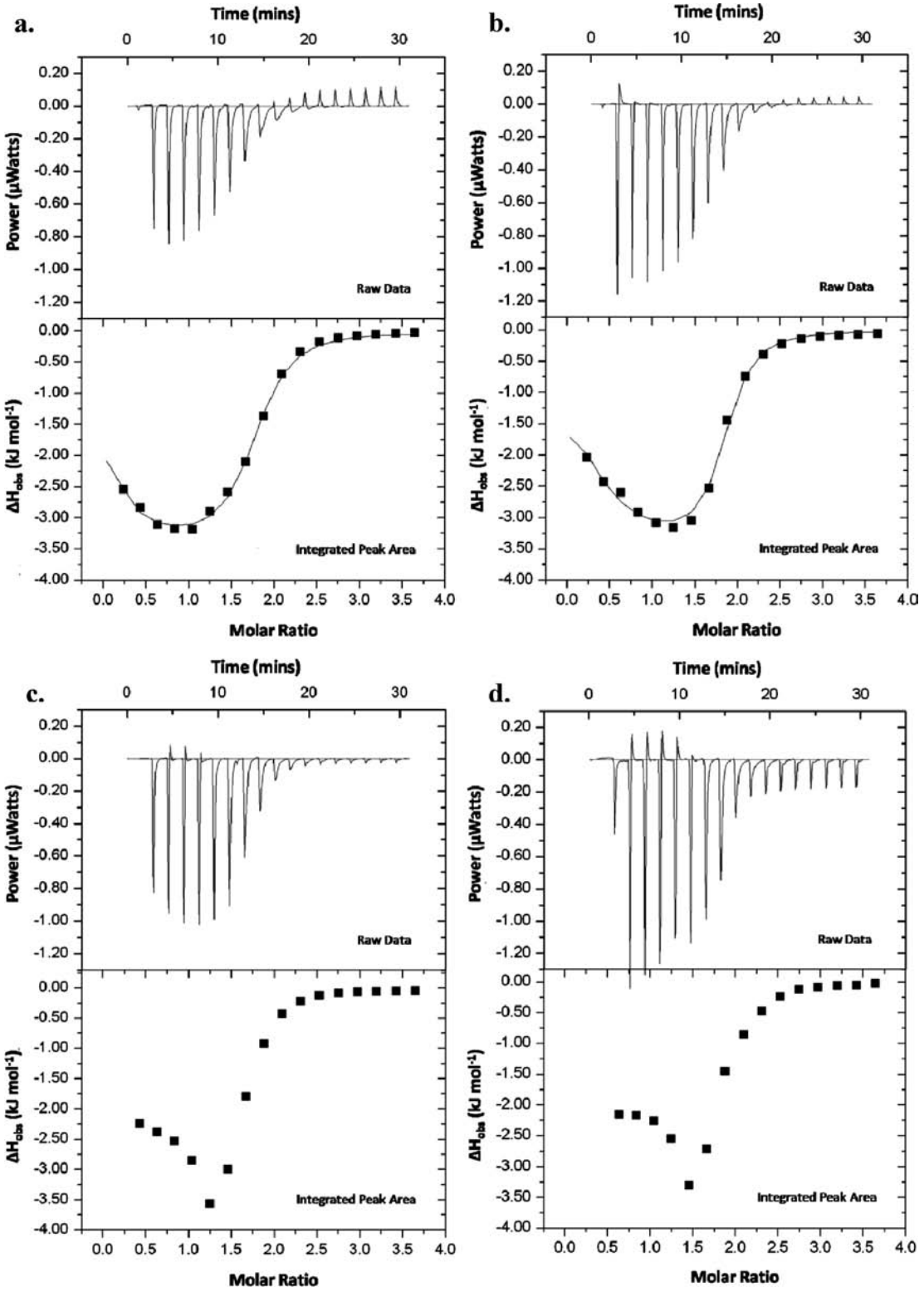

Figure 5. Interaction of preveriason seed tannin with polyproline studied by 10 °C (a), 25 °C (b), 45 °C (c) and 55 °C (d) showing the thermogram and binding isotherm. The fitted lines used the two sets of independent sites model.

Effect of Tannin Age on PLP Interaction. The relative binding constants and changes in enthalpy and entropy indicated that the nature of the PLP−tannin interaction changed with tannin age. This is likely to be due to a number of changes in tannin structure that occur over time. First, the greater incorporation of anthocyanins into the structure of grape tannins after veraison results in an increased proportion of sugar residues and positively charged subunits. This produces a less structured hydration shell around the compound as it hydrogen bonds with the surrounding water molecules and thus potentially reduces the hydrophobic interactions with PLP (*36*). Second, the polymerization of tannins under winelike conditions over time produces greater intramolecular hydrophobic interactions and thus compact conformations (*19*, *32*), leading to fewer available binding sites for PLP association than for grape tannins of the same molecular mass. Compact tannin conformations reportedly have reduced associations

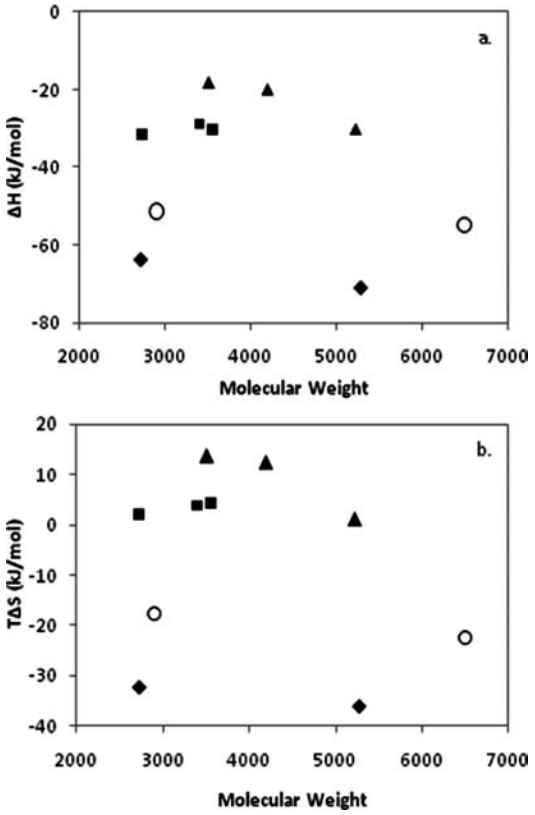

Figure 6. The change in enthalpy (ΔH) (**a**) and change in entropy ($T\Delta S$) (**b**) determined by ITC relative to the average molecular weight of each tannin sample, as determined by GPC. Aged wine tannin (▲); young wine tannin (■); CR grape tannin (○); PV grape tannin (♦).

with proline-based peptides relative to extended tannin conformations, which are able to interact simultaneously with more than one peptide (*20*). This suggests that the compact conformation of aged wine tannins may have limited capacity to cross-link the PLP−tannin complexes, leading to less association. Grape tannins and younger wine tannins are likely to have more extended conformations than aged wine tannins and therefore have a greater number of available binding sites for interaction with PLP interactions as well as cross-linking PLP−tannin complexes.

ITC investigation of the interactions between PLP and grape or wine tannins demonstrated that the initial interactions, which formed PLP−tannin complexes, involved both hydrophobic interactions and hydrogen-bonding, with the relative contribution of each being dependent on tannin structure and thus conformation. Grape tannins had a greater association with PLP, and this was likely to be due to extended conformations leading to more available binding sites, while wine tannins had less PLP associations, potentially as a result of comparatively compact conformations. These results provide preliminary evidence to explain the apparent concentration-independent change in astringency quality of grapes and red wine tannins with age. This has implications in the wine industry as such approaches may provide a better understanding of the impact that techniques such as fruit maturation and micro-oxygenation have on wine astringency.

ABBREVIATIONS USED

CR, commercially ripe; GPC, gel permeation chromatography; ITC, isothermal titration calorimetry; MCP, methyl cellulose polymer; mDP, mean degree of polymerization; PLP, poly (L-proline); PV, preveraison.

ACKNOWLEDGMENT

We thank Dr. Keren Bindon for the isolation of the grape tannins.

LITERATURE CITED

(1) Vidal, S.; Francis, L.; Noble, A.; Kwiatkowski, M.; Cheynier, V.; Waters, E. Taste and mouth-feel properties of different types of tannin-like polyphenolic compounds and anthocyanins in wine. *Anal. Chim. Acta* **2004**, *513*, 57−65.

(2) Es-Safi, N. E.; Fulcrand, H.; Cheynier, V.; Moutounet, M. Studies on the acetaldehyde-induced condensation of (−)-epicatechin and malvidin 3-O-glucoside in a model solution system. *J. Agric. Food Chem.* **1999**, *47*, 2096−2102.

(3) Cheynier, V.; Dueñas-Paton, M.; Salas, E.; Maury, C.; Souquet, J.-M.; Sarni-Manchado, P.; Fulcrand, H. Structure and Properties of Wine Pigments and Tannins. *Am. J. Enol. Vitic.* **2006**, *57* (3), 298−305.

(4) Waters, E. J.; Peng, Z.; Pocock, K. F.; Jones, G. P.; Clarke, P.; Williams, P. J. Solid-state 13C NMR Investigation into Insoluble Deposits Adhering to the Inner Glass Surface of Bottled Red Wine. *J. Agric. Food Chem.* **1994**, *42*, 1761−1766.

(5) Haslam, E. *In Vino Veritas* - Oligomeric Procyanidins and the Aging of Red Wines. *Phytochemistry* **1980**, *19*, 2577−2582.

(6) Vidal, S.; Cartalade, D.; Souquet, J.-M.; Fulcrand, H.; Cheynier, V. Changes in proanthocyanidin chain length in winelike model solutions. *J. Agric. Food Chem.* **2002**, *50*, 2261−2266.

(7) Mercurio, M. D.; Smith, P. A. Tannin Quantification in Red Grapes and Wine: Comparison of Polysaccharide- and Protein-Based Tannin Precipitation Techniques and Their Ability to Model Wine Astringency. *J. Agric. Food Chem.* **2008**.

(8) González-Manzano, S.; Rivas-Gonzalo, J. C.; Santos-Buelga, C. Extraction of flavan-3-ols from grape seed and skin into wine using simulated maceration. *Anal. Chim. Acta* **2004**, *513*, 283−289.

(9) Monagas, M.; Bartolome, B.; Gomez-Cordoves, C. Updated knowledge about the presence of phenolic compounds in wine. *Crit. Rev. Food Sci. Nutr.* **2005**, *45*, 85−118.

(10) Kennedy, J. A.; Hayasaka, Y.; Vidal, S.; Waters, E. J.; Jones, G. P. Composition of Grape Skin Proanthocyanidins at Different Stages of Berry Development. *J. Agric. Food Chem.* **2001**, *49*, 5348−5355.

(11) Kennedy, J. A.; Matthews, M. A.; Waterhouse, A. L. Changes in grape seed polyphenols during fruit ripening. *Phytochemistry* **2000**, *55*, 77−85.

(12) Monagas, M.; Bartolomé, B.; Gómez-Cordovés, C. Evolution of polyphenols in red wines from *Vitis vinifera* L. during aging in the bottle. II. Non-anthocyanin phenolic compounds. *Eur. Food Res. Technol.* **2005**, *220*, 331−340.

(13) Drinkine, J.; Lopes, P.; Kennedy, J. A.; Teissedre, P. L.; Saucier, C. Ethylidene-bridged flavan-3-ols in red wine and correlation with wine age. *J. Agric. Food Chem.* **2007**, *55*, 6292−6299.

(14) Schwartz, M.; Winterhalter, P. Novel aged anthocyanidins from Pinotage wines: Isolation, characterization, and patherway of formation. In *Red wine color—Exploring the mysteries*; Waterhouse, A. L., Kennedy, J. A., Eds.; American Chemical Society: Washington, DC, 2004; pp 179−197.

(15) Cheynier, V. Flavonoids in wine. In *Flavonoids - Chemistry, biochemistry and applications*; Andersen, O. M., Markham, K. R., Eds.; Boca Raton, 2006.

(16) Ferreira, D.; Slade, D.; Marais, J. Flavans and proanthocyanidins. In *Flavonoids - Chemistry, biochemistry and applications*; Andersen, O. M., Markham, K. R., Eds.; CRC Taylor & Francis: Boca Raton, 2006; pp 553−616.

(17) Dinnella, C.; Recchia, A.; Fia, G.; Bertuccioli, M.; Monteleone, E. Saliva characteristics and individual sensitivity to phenolic astringent stimuli. *Chem. Senses* **2009**, *34*, 295−304.

(18) Charlton, A.; Baxter, N.; Khan, M.; Moir, A.; Haslam, E.; Davies, A.; Williamson, M. Polyphenol/peptide binding and precipitation. *J. Agric. Food Chem.* **2002**, *50*, 1593−1601.

(19) Simon, C.; Barathieu, K.; Laguerre, M.; Schmitter, J.-M.; Fouquet, E.; Pianet, I.; Dufourc, E. J. Three-dimensional structure and

dynamics of wine tannin-saliva protein complexes. a multitechnique approach. *Biochemistry* **2003**, *42*, 10385−10395.
(20) Cala, O.; Pinaud, N.; Simon, C.; Fouquet, E.; Laguerre, M.; dufourc, E. J.; Pianet, I. NMR and molecular modeling of wine tannins binding to saliva proteins: revisiting astringency from molecular and colloidal prospects. *FASEB J.* **2010**, *24*, 4281−4290.
(21) Hagerman, A. E.; Rice, M. E.; Ritchard, N. T. Mechanisms of protein precipitation for two tannins, pentagalloyl glucose and epicatechin16 (4f8) catechin (procyanidin). *J. Agric. Food Chem.* **1998**, *46*, 2590−2595.
(22) Pascal, C.; Poncet-Legrand, C.; Imberty, A.; Gautier, C.; Sarni-Manchado, P.; Cheynier, V.; Vernhet, A. Interactions between a non glycosylated human proline-rich protein and flavan-3-ols are affected by protein concentration and polyphenol/protein ratio. *J. Agric. Food Chem.* **2007**, *55*, 4895−4901.
(23) Wu, G.; Lee, K. Y. C. Interaction of poloxamers with liposomes: an isothermal titration calorimetry study. *J. Phys. Chem. B* **2009**, *113*, 15522−15531.
(24) Kennedy, J. A.; Jones, G. P. Analysis of Proanthocyanidin Cleavage Products Following Acid-Catalysis in the Presence of Excess Phloroglucinol. *J. Agric. Food Chem.* **2001**, *49*, 1740−1746.
(25) Bindon, K.; Smith, P.; Kennedy, J. A. Interaction between Grape-Derived Proanthocyanidins and Cell Wall Material. 1. Effect on Proanthocyanidin Composition and Molecular Mass. *J. Agric. Food Chem.* **2010**, *58*, 2520−2528.
(26) Kennedy, J. A.; Taylor, A. W. Analysis of proanthocyanidins by high-performance gel permeation chromatography. *J. Chromatogr., A* **2003**, *995*, 99−107.
(27) Sturtenvant, J. M. Heat capacity and entropy change in processes involving proteins. *Proc. Natl. Acad. Sci. U.S.A.* **1977**, *74*, 2236−2240.
(28) Freire, E.; Mayorga, O. L.; Straume, M. Isothermal titration calorimetry. *Anal. Chem.* **1990**, *62*, A950−A959.
(29) Guyot, S.; Vercauteren, J.; Cheynier, V. Structural determination of colourless and yellow dimers resulting from (+)-catechin coupling catalysed by grape polyphenoloxidase. *Phytochemistry* **1996**, *42*, 1279−1288.
(30) Sun, W.; Miller, J. M. Tandem mass spectrometry of the B-type procyanidins in wine and B-type dehydrodicatechins in an autoxidation mixture of (+)-catechin and (-)-epicatechin. *J. Mass Spectrom.* **2003**, *38*, 438−446.
(31) Le Bourvellec, C.; Guyot, S.; Renard, C. M. G. C. Non-covalent interaction between procyanidins and apple cell wall material: Part I. Effect of some environmental parameters. *Biochim. Biophys. Acta, Gen. Subj.* **2004**, *1672*, 192−202.
(32) Tarascou, I.; Barathieu, K.; Simon, C.; Ducasse, M. A.; Andre, Y.; Fouquet, E.; Dufourc, E. J.; de Freitas, V.; Laguerre, M.; Pianet, I. A 3D structural and conformational study of procyanidin dimers in water and hydro-alcoholic media as viewed by NMR and molecular modeling. *Magn. Reson. Chem.* **2006**, *44*, 868−880.
(33) Poncet-Legrand, C.; Gautier, C.; Cheynier, V.; Imberty, A. Interactions between flavan-3-ols and poly(L-proline) studied by Isothermal Titration Calorimetry: Effect of the tannin structure. *J. Agric. Food Chem.* **2007**, *55*, 9235−9240.
(34) Jelesarov, I.; Bosshard, H. R. Isothermal titration calorimetry and differential scanning calorimetry as complementary tools to investigate the energetics of biomolecular recognition. *J. Mol. Recognit.* **1999**, *12*, 3−18.
(35) Ladbury, J. E. Calorimetry as a tool for understanding biomolecular interactions and an aid to drug design. *Biochem. Soc. Trans.* **2010**, *38*, 888−893.
(36) Haslam, E. Natural polyphenols (vegetable tannins) as drugs: Possible modes of action. *J. Nat. Prod.* **1996**, *59*, 205−215.

Received for review August 10, 2010. Revised manuscript received October 27, 2010. Accepted October 27, 2010. The AWRI, a member of the Wine Innovation Cluster in Adelaide, is supported by Australia's grape growers and winemakers through their investment body, the Grape and Wine Research Development Corporation, with matching funds from the Australian government. R.J.F. was supported by the National Collaborative Research Infrastructure Strategy, an Australian Federal Government initiative.